

Islands as Nanometric Probes of Strain Distribution in Heterogeneous Surfaces

H. Realpe,^{1,3} E. Peretz,¹ N. Shamir,^{2,*} M. H. Mintz,^{2,3} R. Z. Shneck,⁴ and Y. Manassen¹

¹*Department of Physics and the Ilse Katz Institute for Nanoscale Science and Technology, Ben-Gurion University of the Negev, P.O. Box 653 Beer-Sheva, 84104, Israel*

²*Nuclear Research Center-Negev, P. O. Box 9001 Beer-Sheva, 84190, Israel*

³*Department of Nuclear Engineering, Ben-Gurion University of the Negev, P. O. Box 653 Beer-Sheva 84104, Israel*

⁴*Department of Materials Engineering, Ben-Gurion University of the Negev, P.O. Box, 653, Beer-Sheva, 84105, Israel*

(Received 18 November 2009; published 5 February 2010)

Many of the surface phenomena are driven by elastic energy and elastic interactions. Despite the fact that there are many microscopic techniques with nm and atomic resolution, an established technique to study the distribution of strain on the surface is still lacking. We present a study on the Gd(0001)/W(110) system, in which undulations in the Gd layer are detected by STM. This creates a heterogeneous surface with reduced strains, due to relaxation, on the crests of the waved surface and elevated strains in the troughs. An additional part of the strain is released through Stransky-Krastanov growth of Gd islands. Utilizing a strain-relief model, we show that the island size and shape reflect the strain variations on the surface. Strain maps were calculated, using the island as nanoprobe, with good correlation to the surface topography.

DOI: 10.1103/PhysRevLett.104.056102

PACS numbers: 68.60.Bs, 68.37.Ef

Islands are nucleated on a strained surface as part of the mechanism of strain relief. Their parameters are a function of the local strain, originating from the surface topography. In the present study we present a method of using the island parameters to probe this local strain and draw strain maps that are in correlation with the topography of the surface.

The equilibrium shape of a stress-free solid body is governed by minimization of its total surface energy. For a single crystal, the minimum energy is associated with a faceted shape, the faces being parallel to certain low index crystallographic planes [1]. As a result, any roughening of the surface will lead to an increase in the surface energy and will result in mass transport that will flatten the corrugation.

When the surface is subject to external stress, the total energy to be minimized includes the elastic energy. A flat thin layer surface, subjected to epitaxial stresses, due to interface misfit between the layer and substrate, may develop topographic undulation due to kinetic, or Asaro-Tiller-Grienfeld (ATG) instability, beyond a critical stress [2–4]. The stresses on the crests of the undulated surface are relaxed, relative to the “valleys,” leading to a total reduction of the surface strain energy. Hence, a periodic strain field is created, with maximum-minimum values that coincide with the peak-valley pattern of the undulation.

Another mechanism of strain relaxation is the Stransky-Krastanov (SK) growth mode [5]. In this growth mode, an epitaxial thin film is grown on a substrate which has a lattice mismatch with the film. Initially, the film is grown in a layer by layer mode. After passing a critical thickness, it turns into a three-dimensional growth, where islands are formed on top of the stressed wetting layer. The driving force for the formation of the 3D islands is the fact that

they can release part of the stress that depends of the shape of the island. Namely, the larger the aspect ratio $r = h/l$ (when h is the height of the island and l is its radius) the more efficient is the stress relaxation. Because of the so-generated heterogeneous strain, island nucleation is heterogeneous [6]. In the present Letter we report on a case where both kinetic instability (possibly ATG) and SK growth were invoked to relax epitaxial stresses and we show that such observation can be utilized to probe the local strains across the surface.

We have performed an STM study on the Gd(0001)/W(110) system. It has been reported [7,8], that the first monolayer of Gd on the W(110) surface possesses a strained hcp structure with a significant dilatation (of about 8%, according to Ref. [7], or about 2% according to Ref. [8]), due to the lattice mismatch of the two materials planes.

A W(110) crystal served as the substrate for the growth of the Gd islands. An STM UHV chamber (backpressure $\sim 10^{-8}$ Pa) equipped with Auger Electron Spectroscopy (AES) was utilized. The crystal was cleaned by repeated cycles of heating at 1760 K in oxygen and flashing up to 2600 K. These cycles were repeated until the carbon AES signal, appearing at the end of the flashing stage stabilized to a relatively low value (of a few percent). The STM image of such a clean W(110) surface displayed a terrace pattern, with terrace widths in the range of 0.03–0.15 μm . The Gd films were deposited by means of an e -beam evaporator. During Gd deposition the pressure raised up to 1×10^{-7} Pa. The initial deposition was controlled to produce coverage of 5–20 monolayers. The surface of the sample was characterized by AES and the sample was then annealed at 920 K during 9–16 min. During this annealing,

the homogeneous deposited layer turned into an island pattern, by the SK process [5]. The sample was then cooled down to room temperature, analyzed again by AES and imaged by STM. The final heights of the islands were in the range of 2–6 nm, with a thin layer of Gd between them.

Some regions of the surface displayed a clear roughening process that resulted in surface undulations. The undulation wavelength and amplitude are found to be in the range of 0.5–3 μm and 4–10 nm, respectively. Figure 1(a) shows two examples for such undulated surfaces. The initial coverage of the Gd film was 16 (left) and 11 (right) monolayers.

As displayed in Fig. 1(a), in addition to the undulation of the surface, 3D islands of Gd are formed with different sizes. However, it is easy to see that the size and shape of the islands are not random but depend on their location relative to the underlying undulation, as can be observed in Fig. 2 that presents V vs r for both undulated surfaces presented in Fig. 1(a). The values for peak islands and valley ones are indicated by full and empty dots, respectively.

The presence of islands on the surface indicates that the undulations were unable to relax all the stress on it. Hence, the residual strain gives rise to the SK growth mode of islands. Moreover, the tensile stresses that prevail at the crests on the surface are now smaller and stresses prevailing in the troughs are larger than for the initial, evenly deposited layer. Therefore, the size and shape of the different islands on the layer may be assumed to adjust to this difference. Since the islands are large and the heating time

was long, we assume that these islands are at equilibrium, and their shape is determined by energy considerations. Thus we suggest that the islands may serve as sensors of the local strain across the surface.

The simplest expression of the total energy of the island is given by [5,9,10]. In this expression, the island is assumed to have a box shape. The square base of the box has an area of l^2 and the height of the island is h . Thus the total surface energy is $4lh\gamma$ where γ is the surface energy of Gd. The area of the top of the island (l^2) is not taken into account, since it is counterbalanced by the elimination of the interface at the basal plane. The elastic energy due to 2D tension in an epitaxial layer is given in [10] by: $[E/(1 - \nu)] \cdot V \cdot \varepsilon^2$ where E is the Young modulus of Gd, ν its Poisson ratio, V is the volume of the island, and ε is the natural (original) misfit between the island's base and the island (i.e., natural Gd). An island that grows above the epitaxial base layer is relaxed relative to that layer, hence its elastic energy is reduced by a factor $R(r)$, varying between 0 and 1, that depends only on the aspect ratio $r = h/l$. Hence, the total energy per unit volume of the island as a function of its volume $V = l^2 \times h$ and aspect ratio, r , is given by:

$$\frac{E(r, V)}{V} = \alpha r^{1/3} V^{-1/3} + \beta \varepsilon^2 R(r), \quad (1)$$

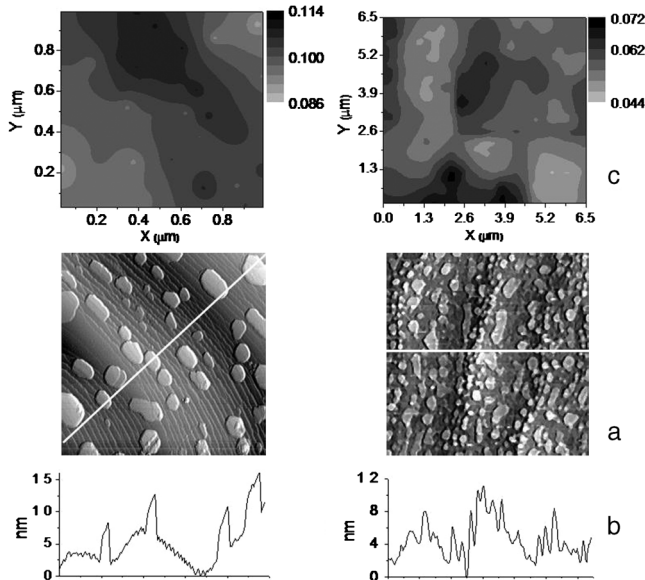


FIG. 1. (a) STM images of Gd(0001)/W(110). These images are of areas: left—1 μm^2 ; right—6.5 μm^2 . (b) Height profiles (along the white lines) for both images at (a). (c) Strain maps (evaluated as described in the text) for both images at (a). The strain scale is given at the right side of the map.

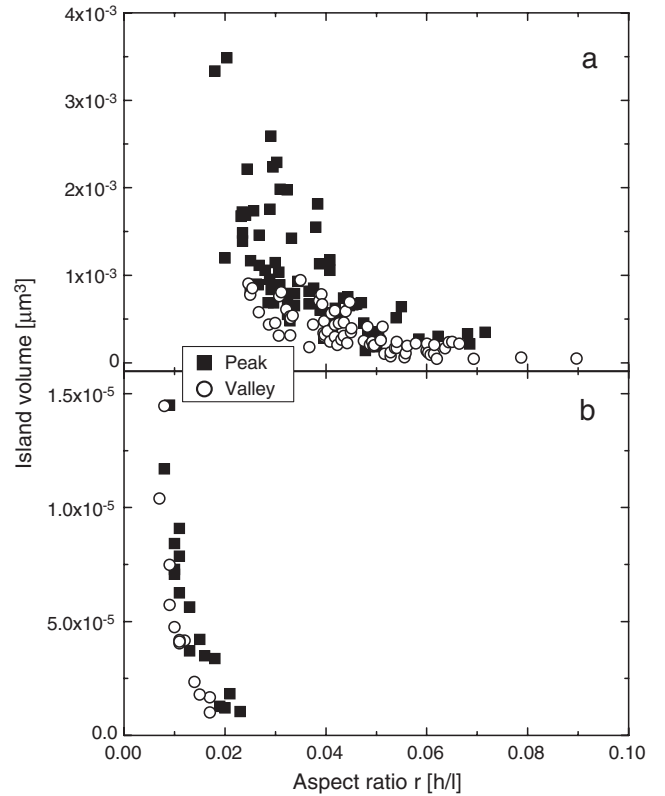


FIG. 2. Volume of the island vs aspect ratio for the islands in the images in Fig. 1(a): (a) right side image—6.5 μm^2 ; (b) left side image—1 μm^2 .

with $\alpha = 4\gamma$ and $\beta = E/(1 - \nu)$. $R(r)$ is a monotonic decaying function of r ranging from 1 at $r = 0$ to 0 at large r . The first term in the above equation favors as small as possible r and complete wetting of the surface. The second term favors the three-dimensional growth of the islands to enable relaxation with r as large as possible. Thus, for a given value of ε , the energy density will have a minimum. This value can be calculated when the function $R(r)$ is known. We take the simplest form given by Kern and Müller (Fig. 12 in Ref. [9], for $K = 1$, since the elastic properties of the island and the surface are the same). The curve $K = 1$ was fitted to a power law formula: $R(r) = -1.17r^{0.28} + 1.12$ for $0 < r < 0.85$.

In principle the energy density per unit volume is a function of both V and r . However these two variables do not seem to be independent, as can be observed in Fig. 2. An exponential function of the form:

$$V(r) = A + Be^{-(r/C)} \quad (2)$$

was fitted to each graph. Thus, the energy density can be written as a function of V only. Taking the derivative with respect to V and equating to zero allows us, after some mathematical manipulation, to express ε as:

$$\varepsilon = \left[\frac{C^{0.053} \alpha}{\beta} \right]^{1/2} \left[\frac{V + \left(\ln \left| \frac{B}{V-A} \right| \right) (V-A)}{V^{4/3}} \right]^{1/2} \times \left(\ln \left| \frac{B}{V-A} \right| \right)^{0.0265}. \quad (3)$$

Substituting the properties of Gd, namely, $E = 6 \times 10^{10} \text{ N/m}^2$, $\nu = 0.259$ and $\Gamma = 1.23 \text{ J/m}^2$ [11] and the volumes of the islands, gives the values of the original or natural misfit strain between the Gd islands and the stressed inhomogeneous Gd surface at each island position. These values of strain can be used in order to construct a map of the distribution of strain on the surface. The strain value found for each location of the island was attributed to all the pixels that are closer to this island than to other ones.

The distribution of the strain of the two surfaces regimes of Fig. 1(a), in correlation to the topography, is shown, respectively, in Fig. 1(c). A qualitative correlation of the strain map to the surface topography is clearly depicted.

The ATG instability has an expression for the critical surface undulation wavelength λ_c [5]:

$$\lambda_c = \frac{\pi\gamma}{\sigma^2} \frac{E}{1 - \nu^2} = \frac{\pi\gamma}{E\varepsilon^2} \frac{1}{1 - \nu^2} \Rightarrow \varepsilon \propto \frac{1}{\lambda^{1/2}}, \quad (4)$$

where σ is the stress concentration.

Figure 3 presents the experimental average strain for peak and valley islands in all 12 undulated regions that were measured (including six flat ones, strains: 0.023–0.056, averaged as one point), vs $\lambda^{-0.5}$. It can be clearly seen that in all undulated cases, the valley average strain is larger than the peak one and the general trend is not far from linear increase in strain with $\lambda^{-0.5}$, which indicates a possibility of ATG instabilities. Calculations, using finite

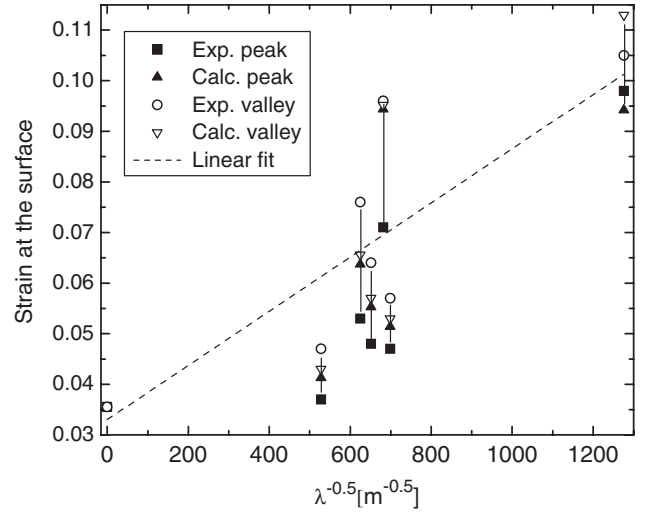


FIG. 3. Calculated (from average, measured, island parameters) strain at the surface, vs $\lambda^{-0.5}$, for all measured surfaces (including 6 “flat” ones, averaged), together with the calculated (by finite elements, for the same λ , amplitude and average strain) values. The vertical lines indicate icons of the same surface. The straight line is the linear fit for the experimental values.

elements performed on each surface (using its wavelength, amplitude and average strain of each surface map) are also presented in Fig. 3. They yielded similar results, with a much smaller difference in strain between peak and valley (except one case), probably because the calculation does not take into account the contribution of the formed islands to strain relief.

It is clear that the size and shape of the islands depend on the misfit strain and therefore the islands’ volume and aspect ratio provide a generally consistent image of misfit strain relative to the underlying layer. In particular, we note the following. (a) In the higher parts of the undulations the misfit strain is smaller; this allows the islands to grow larger in volume. Concurrently the aspect ratios of the islands are smaller, since they have smaller strain to relax. (b) In the lower parts of the undulation the strain is larger. The largest values are found where the trough radius of curvature is the smallest. The aspect ratios of the islands are large to allow efficient strain relaxation. (c) The two images presented and all their relevant parameters are very different: $\lambda \sim 0.5 \mu\text{m}$ (left) vs $\sim 2.5 \mu\text{m}$ (right) and a factor of ~ 100 between islands sizes (Fig. 2) and most important—different strain ranges, consistent with both earlier observations [7,8]. The reason may be local high strain at the left that forced the short wavelength and island sizes for optimal relief, or other initial parameters (like local substrate structure, not known to us). (d) For the flat areas, an average strain of 3.55% was obtained, strengthening the hypothesis that the undulated structures were induced by high local strains, in order to relieve them.

Presently it is hard to estimate the precision of these strain maps. However, this can be improved in several

ways: we have made a crude approximation that the islands are box shaped (and took into account only islands that have a shape close to a box). It is possible to improve the model by making a more precise estimation of the surface energy term and the elastic relaxation term that depends sensitively on the shape of the island. As an example we tried to use the derivation given in Ref. [12] for a trapezoidal island which has an angle different than 90° with the surface. The results were not very much different than those of the box shaped islands. Also, we ignore the dependence of the surface energy on the stress and the curvature. In addition, the islands themselves are expected to modify the local strain. A previous study [13], demonstrates the possible size effect of mismatch between the islands and the substrate beneath it, which also contributes to the inability of precisely probing the local strain on the surface.

To summarize, we have shown that in surfaces with modulated strain, the islands that grow as a result of this strain reflect with their volume and aspect ratio the local level of strain. We applied a well-known simple model to evaluate quantitatively the level of strain, and observed the expected dependence of the size and shape on the misfit strain.

The fact that the strain distribution is consistent with the topographic image clearly indicates that the strain between the surface and the island is the dominant if not the only parameter that determines the island volume and the aspect ratio. Moreover, it indicates that the simple model used, describes correctly the energy of the islands. This justifies *a priori* the use of the volumes and aspect ratios for the

estimation of the strain, and indicates the reliability of these strain maps.

This estimation of the strain distribution in heterogeneous surfaces is also important in an ongoing study of the effect of strain on chemical reactions on surfaces.

This work was partially supported by a grant from the Israel Council for Higher Education and the Israel Atomic Energy Commission and a grant from the Ministry of National Infrastructure, Division of R&D.

*Corresponding author.

noah.shamir@gmail.com; Fax: 972-8-6568751

- [1] B. Salanon and P. Hecquet, Surf. Sci. **412–413**, 639 (1998).
- [2] R. Asaro and W. Tiller, Metall. Trans. **3**, 1789 (1972).
- [3] M. Grienfeld, Sov. Phys. Dokl. **31**, 831 (1986).
- [4] D. Srolovitz, Acta Metall. **37**, 621 (1989).
- [5] P. Müller and A. Saul, Surf. Sci. Rep. **54**, 157 (2004).
- [6] A. Bourret, Surf. Sci. **432**, 37 (1999).
- [7] D. Weller and S.F. Alvarado, J. Appl. Phys. **59**, 2908 (1986).
- [8] S.A. Nepijko, M. Getzlaff, R. Pascal, Ch. Zarnitz, M. Bode, and R. Wiesendanger, Surf. Sci. **466**, 89 (2000).
- [9] R. Kern and P. Müller, Surf. Sci. **392**, 103 (1997).
- [10] P. Müller and R. Kern, J. Cryst. Growth **193**, 257 (1998).
- [11] in *Chemical Rubber Company Handbook of Chemistry and Physics*, edited by D.R. Lide (CRC Press, Boca Raton, Florida, USA, 1998), 79th ed..
- [12] J. Tersoff and R.M. Tromp, Phys. Rev. Lett. **70**, 2782 (1993).
- [13] P. Müller, P. Turban, L. Lapena, and S. Andrieu, Surf. Sci. **488**, 52 (2001).